Reference Soret coefficients of natural isotopes and diluted alloys of tin

S. Van Vaerenbergh,[1] J. P. Garandet,[2] J. P. Praizey,[2] and J. C. Legros[1]

[1]*Université Libre de Bruxelles, Chemical Physics EP, CP 165, 50 Franklin Delano Roosevelt Avenue,*
1050 Brussels, Belgium

[2]*Commissariat à l'Energie Atomique, CEA/DTA/CEREM/DEM, Section d'Etudes de la Solidification, 17 rue des Martyrs,*
38054 Grenoble Cedex 9, France

Measurements of Soret coefficients of tin alloys have been performed in the MFA-067 experiment of the automatic retrievable satellite EURECA. They complete the set of measurements performed in tin dilute alloys in microgravity manned laboratories. They allow also for an accurate determination of the isotopic thermomigration and for a better evaluation of the accuracy of microgravity measurements of the thermodiffusion factors. These data are compared to nonequilibrium condensed matter theories. A reasonable agreement has been obtained with the revised Enskog theory, and no electronic contribution could be identified. [S1063-651X(98)10208-8]

I. INTRODUCTION

The Soret coefficient and thermodiffusion factor of the considered elements are here defined from the following phenomenological expression of the mass diffusive flux:

$$\mathbf{J} = -\rho D \boldsymbol{\nabla} C - \rho D_T C \boldsymbol{\nabla} T, \quad (1)$$

where ρ, T, and C are respectively the density, temperature, and mass fraction of the solute and where D and D_T are the isothermal diffusion and thermodiffusion coefficients of the solute. Such an expression of the diffusive flux is valid for dilute solutions [1,2]. As a result, in the absence of convection and in a thermal gradient established between two impervious boundaries, the Fickian and thermodiffusive fluxes balance. Then,

$$\boldsymbol{\nabla} \ln(C) = -\frac{D_T}{D} \boldsymbol{\nabla} T = -k_T \boldsymbol{\nabla} \ln(T). \quad (2)$$

The ratio D_T/D is the Soret coefficient of the solute and k_T the thermodiffusion factor of the solute (some authors define it with the opposite sign). They may depend on temperature and mass fraction. For metallic alloys, the thermodiffusion factor is of the order of unity, and may be positive or negative.

Thermomigration is recognized as a preponderant effect, for instance, in processes involving electron or laser beam heating. It is also used in the industrial process of thermodiffusive coating. Under small temperature gradient, in a purely conductive state, thermodiffusion does not induce large compositional gradients, and is frequently omitted in the description of nonisothermal processes for this reason. However, even with weak thermal gradients, this may be erroneous because, due to the large dependence of the physical parameter on composition, it strongly influences among others the morphological stability of the solidification front and the hydrodynamical stability.

As a consequence of hydrodynamic instabilities and Rayleigh convection, it is difficult to measure on ground conditions. The microgravity measurements of the Soret effect appeared to be an essential tool after the first such measurement performed in a dilute solution of cobalt in tin during the First SpaceLab Payload (FSLP) mission [3]. A large value of the thermodiffusion factor has been obtained and no Soret effect could be detected in the ground based measurement, although the shear cell was *a priori* designed to minimize the natural convection [4].

In the shear cell technique, the liquid samples are processed in capillaries by the imposed axial thermal gradient. The capillaries are achieved in a superposition of disks that are rotated on their common axis once the chemical separation is established, thus dividing the liquid veins in as many samples as disks. The quenching method uses the same geometry, but it studies the thermomigration of a radioactive layer sandwiched between nonradioactive material. In the latter the drift that appeared in the diffusing layer is analyzed after quenching of the overall capillary.

The shear cell technique presents the advantages that it can be used for any metallic system and that the experiments are performed in well-defined thermal conditions. For this reason, it has been selected for a systematic campaign of measurements in tin alloys in both normal and satellite gravity levels. After the FSLP mission, results have been obtained in the First German Spacelab mission (D1 mission) [4,5] in tin diluted solutions of argentum, bismuth, and natural isotopic mixture of pure tin. The comparison with ground based measurements showed that the convection could be to some extent slowed down by a stabilizing solute gradient.

The long duration of very low gravity level of the European Retrievable Carrier EURECA 1 mission performed in 1992–1993 allowed the use of longer capillaries. This opportunity has been used [6] in the MFA067 experiment to obtain an accurate determination of the isotopic thermomigration in three isotopes of tin. Also, a measurement performed in a more concentrated solution of gold in tin has completed the experimental data needed to test the theoretical model evaluating the effect of convective transport on the chemical separation in capillaries.

TABLE I. Measurements of thermodiffusion factors in liquid tin: experimental setup (defined in Table III), mass fraction, estimated accuracy of the measurements, thermodiffusion factor, and experimental standard deviation (see the text).

Set-up solute	C_0 (weight %)	Accuracy (%)	$10^3 k_T$	Standard deviation (%)
FSLP Co	4.0×10^{-2}	17	1860 ± 40	2.2
D1 ^{112}Sn	natural composition	39	77 ± 8	10
D1 Ag	4.0×10^{-2}	26	175 ± 49	29
D1 Bi	4.0	18	-758 ± 66	9
EURECA (cap. 3)	natural composition			
^{112}Sn		23	73 ± 7	10
^{116}Sn		38	24 ± 5	21
^{124}Sn		28	-51 ± 7	14
EURECA (cap. 1)	natural composition			
^{112}Sn		23	80 ± 8	10
^{116}Sn		38	41 ± 8	20
^{124}Sn		28	-60 ± 10	17
EURECA (cap. 4) Au	7.0×10^{-2}	9	-837 ± 12	1.4

So, it is now possible to quantify all the known sources of errors of the microgravity measurements and we shall evaluate the accuracy of all the above mentioned measurements in tin alloys. The data so collected and evaluated allow one to assess the predictive capability of the nonequilibrium theories.

II. SYSTEMS STUDIED, COMPOSITION MEASUREMENTS AND SETUP CHARACTERISTICS

The tin systems studied in microgravity are listed in Table I. The purity of the products used is better than 5 ppm. The measurements in the capillary 2 of the MFA067 experiment are not taken into account because of a leakage that occurred during the experiment.

Except for the Bi-Sn system, analyzed by an atomic absorption spectroscopy [4], the composition of the samples has been obtained by neutron activation in the French SILOE reactor of CEN-G (Grenoble). The samples have been rotated with the fluence calibration sample at constant angular velocity in the neutron exposition chamber. This technique

TABLE III. Column 1: the denomination of the setup, all used in both ground based measurements and microgravity measurements, with the name and the year of the flight mission; column 2: the material of the disks and their number N; column 3: the dimensions in millimetres of the capillaries (diameter, total length); column 4: the mean temperature (in kelvin); column 5: the measured axial temperature difference (in kelvin); column 6: the estimated radial temperature difference (in centikelvin).

Setup	Number and material of disks	$d*L$ $(mm*mm)$	T_0 (K)	ΔT_{ax} (K)	ΔT_{rad} (K) $(\times 100)$
GHF on FSLP 1983	6 zirconia	$2*18$	773	500	2
GHF on D1 1985	6 zirconia	$2*18$	773	500	2
MFA on EURECA 1993–1994	11 alumina	$2*110$	823	460	2

provides a very accurate measurement of the compositions, estimated to be better than 0.5% for all the measurements. The following nuclear reactions have been considered for the composition analysis:

$$^{112}Sn(n,\gamma)^{113}Sn, \quad \gamma=0.392 \text{ MeV}, \quad 115 \text{ days}$$
$$^{116}Sn(n,\gamma)^{117}Sn, \quad \gamma=0.159 \text{ MeV}, \quad 14 \text{ days}$$
$$^{124}Sn(n,\gamma)^{125}Sn, \quad \gamma=1.067 \text{ MeV}, \quad 9.6 \text{ days}$$
$$^{59}Co(n,\gamma)^{60}Co, \quad \gamma=1.17 \text{ and } 1.33 \text{ MeV}, \quad 5.3 \text{ years}$$
$$^{197}Au(n,\gamma)^{198}Au, \quad \gamma=0.411 \text{ MeV}, \quad 2.7 \text{ days}$$
$$^{109}Ag(n,\gamma)^{110}Ag, \quad \gamma=0.657 \text{ MeV}, \quad 250 \text{ days}$$

The neutron activation does not provide helpful reactions for the other Sn isotopes. The natural abundance of tin isotopes is reported in Table II.

The characteristics of the shear cells used are given in Table III. For the scope of evaluating the convective perturbations, the same shear cells have been used in ground based and in microgravity measurements. In any case, the thermal conductivity of the disks should be close to that of the sample in order to minimize the lateral thermal gradients and the resulting convective perturbations due to buoyancy. Such an objective is not compatible with low power budget of microgravity experiments and the traded off material used is given in Table III. The diameter of the capillaries has been minimized in order to reduce the amplitude of the Rayleigh convection, up to the limit allowed by the filling and the composition analysis. The resulting amplitude of the lateral

TABLE II. Sn isotopes natural abundance: atomic mass in the first row, and atomic mass fraction (in thousands) in the second row. The mean molar mass is 118.69.

Atomic mass		114	115		117	118	119	120	122	
	112			116						124
Mass fraction		6.5	3.4		75.7	240.1	85.9	329.7	47.1	
(in thousands)	9.5			142.4						59.8

thermal gradient, evaluated by two-dimensional numerical simulation, is given in Table III.

The axial thermal gradients have been monitored by thermocouples located in the disks. The accuracy of the measurements are better than 1 K, although the uncertainty resulting from their dimension and axial positioning may be much larger. The linearity and stability of the smoothed thermal profile are, however, better than 1%, except in the extremities' samples.

III. EXPERIMENTAL RESULTS AND ACCURACIES

The results obtained in FSLP and D1 experiments have been reported in detail elsewhere [3–5]. They are summarized with the results obtained for MFA-067 [6,7] in Table I. In all cases, the same experiment performed on ground gives smaller values of k_T. We emphasize in this section the experimental accuracy obtained by considering *in extenso* several causes of errors.

Natural convection in the fluid phase, due to the interaction of the density gradients with gravity, is one obvious potential cause of error.

In dilute alloys, only thermal convection is to be considered, whereas thermal and solutal effects combine in more concentrated systems. In all cases, the additional transport induced by the fluid flow was seen to scale with the square of the non-dimensional Péclet number WH/D, where W and H are the average convective velocity and a typical dimension of the capillary [8,9], here its diameter D.

On Earth, the experimental setup is maintained in as vertical position as possible, so that the radial density gradients act as convective driving force. Even though the radial temperature differences listed in Table III appear to be very small, the non-dimensional Péclet number WH/D takes much higher values [9] than in microgravity.

The solutal destabilization of the flow may take place when the heavier component diffuses upwards, explaining the large discrepancies in the measured one g to zero g thermodiffusion factors, especially for concentrated solutions. On the contrary, when the heavier component migrates downwards, it can provide some stabilization. However, the results shows that even a high solutal stabilization is not sufficient to guarantee purely diffusive mass transport [9].

By the knowledge of the thermodiffusion factor, it is now possible to obtain a clear picture of this stabilizing or destabilizing effect, but such an explanation lies out of the scope of this paper (see [8,9]). It is practically not yet achievable to deduce the thermodiffusion factors from the ground based measurements.

In space, the axial density gradients interact mainly with the component of the residual gravity normal to the capillary axis to give birth to a much reduced, but nonvanishing, fluid flow. However, using standard formulas for fluid velocity, it is possible to show that the relative error induced by convection is smaller than 1% in space when the gravity level is reduced by a factor 10^4 with respect to its ground value g_0 [9].

Such a reduction is typical of what can be obtained in manned shuttle flights such as FSLP and D1. On an automatic platform like EURECA, the accelerometers located on the satellite showed that the gravity level was lower than $10^{-5}g_0$ for frequencies less than 50 Hz. The convection induced relative error should then be vanishingly small in that case [9].

The rate of attainment of the steady state must also be taken into account in the evaluation of the accuracies. In a purely diffusive process the evolution of the solute profile is governed by molecular diffusion [1], so that 98.7% of the steady state is reached after 3τ where

$$\tau = \frac{L^2}{\pi^2 D},\qquad(3)$$

L being the distance between the differentially heated impervious walls. For experiments performed on board satellites, this high processing time limits the allowed length of the capillary. Taking the most unfavorable case of $D = 10^{-5}$ cm^2/sec (see [10]), this rate is higher than 99%. It would have to be reconsidered if the foreseen microgravity measurements of isothermal diffusion coefficients provide much smaller values than the previous ground based measurements.

To these systematic experimental errors, linked to the processing conditions of the samples, are to be added the errors due to the accuracy on the composition analysis and on the temperature sensing. The accuracy of the implemented neutron activation technique is better than 1 ppm if the geometry of exposition is perfectly defined. Given the uncertainty on the cylindricity of the samples (autoabsorption corrections on the fluence), the relative errors on composition measurements are smaller than 0.3% in the worst case of ^{116}Sn for the EURECA samples and 0.5% for FSLP and D1 samples. For bismuth, the composition is performed by atomic absorption spectroscopy, with an accuracy of 1%.

On EURECA, the relative accuracy on the temperature measurements, including the possible mispositioning of the measurement probes, is around 1.4% whereas it is about 2.8% in D1 and FSLP, due to the reduced dimensions of the samples. Assuming that there is no variation of the thermodiffusion factor in the investigated temperature and composition range, the accuracy of the profile analysis is computed with the formula

$$\left|\frac{\delta k_T}{k_T}\right| \leq \left[\left[\left|\frac{1}{k_T}\frac{\delta C}{C}\right| + \left|\frac{\delta T}{T}\right|\right]\right]\left|\frac{1}{\ln(T/\bar{T})}\right|,\qquad(4)$$

where the overbars stands for mean values, and where the error on the mean temperature as been neglected.

The global accuracies of the values of the thermodiffusion factors, estimated taking into account all the above mentioned effects summarized in Table IV, are given in the third column of Table I. These reference measurements are to be given with these computed accuracies.

To strengthen the reliability of the microgravity measurements, it is enough to compare the results obtained for the thermodiffusion factors of ^{112}Sn in pure tin: although very small, their values obtained in microgravity with different shear cells and in different experiments do not vary by more than 10%.

TABLE IV. Data for the error analysis. The durations of experiment correspond to an established thermal profile.

	EURECA	FSLP and D1
Rate of attainment of the asymptotic separation	1%	1%
(duration of the experiment)	(250 h)	(6 and 7 h)
Residual gravity convective perturbation	1%	5%
Temperature measurements	1.4%	2.8%
Composition measurements	0.3%	0.5%[a]

[a]Excluding Bi composition obtained by chemical analysis.

IV. COMPARISON WITH THEORETICAL MODELS

Standard deviations from the fitting laws (2) were evaluated for each capillary in our data base. They are smaller but of the same order as the computed accuracies and this proves that the sources of error of the measurements are well understood. Within these accuracies, the phenomenological law (2) is verified with thermodiffusion factors showing no dependence on temperature or composition.

The amplitude and signs of these reference measurements of thermomigration are valuable inputs to test the predictions of nonequilibrium theories of condensed mater and *vice versa*, that the latter can provide information on the nature of interactions and of the structure of the fluid, as shown below. This possibility arises because the thermodiffusion coefficient has shown in the kinetic theory of gases [11] to be much more sensitive to the long range interactions than the viscosities, isothermal diffusion coefficients, thermal and electrical conductivities.

It is not yet clear if there exists a theory that can precisely predict the Soret coefficients measured in microgravity. Such theories should probably be refined step by step, and we shall try to provide some guidelines with the available theoretical models.

One main input in this task has been the accurate measurement of the isotopic thermomigration allowed by the increased sensitivity of the EURECA experiment. Due to the longer duration of microgravity conditions, it has been possible to measure also the isotopic thermomigration of the ^{116}Sn and ^{124}Sn and this allows for an accurate verification of the isotopic thermomigration law.

A. Analysis with the kinetic theories

The first theory accounting for thermodiffusion is the kinetic theory of gases developed by Chapman and Cowling [11] for nonhomogeneous states. Extensive developments can be found in [12], for instance. They are performed under the assumptions that only binary collisions of classical particles are to be taken into account and that, out of the interaction range, the one particle distribution function is not perturbed with respect to the local Boltzmann distribution. Its application to gases seems completely justified because a large class of interaction potentials can be considered. The dissipative coefficients can be obtained with the desired accuracy through the Sonine expansions. The second order Sonine expansion is required for the evaluation of the thermo-

TABLE V. Ratios of the thermodiffusion factor measured in microgravity to the one obtained by the elastic spheres model.

Element	^{59}Co	^{109}Ag	^{112}Sn	^{116}Sn	^{124}Sn	^{197}Au	^{209}Bi
$R^{\text{exp. micr.}}$	6.2	4.6	3.0	3.3	2.7	3.8	3.0

diffusion coefficients, and the agreement with experiments is recognized as being better than 5% for simple gases.

For reasons shown below, we shall in this section consider only models with hard core collisions. For this simplest model of interaction, it is predicted that the thermodiffusion ratio is proportional to the reduced mass

$$\mu = \frac{m_1 - m_2}{m_1 + m_2} \qquad (5)$$

with a proportionality coefficient of 105/118, that is

$$k_T^{\text{hc}} = -\frac{105}{118}\,\mu. \qquad (6)$$

The validity of such a model is considered as limited to dilute gases. However, the result expressed by formula (6) is a starting point to compare the several theoretical and experimental values of the thermodiffusion factor. They shall be compared to the hard core model of gases by the ratio R defined by

$$R = \frac{k_T}{k_T^{\text{hc}}}. \qquad (7)$$

The data obtained by microgravity measurements are summarized in Table V.

Figure 1 illustrates the experimental results obtained for the tin isotopes. For this group, the mean experimental value of R is 3.0 ± 0.3 and one sees how the gas approximation gives erroneous amplitude. This value is larger than, but of the same order as, that of 2.20 measured by Rutherford for carbon disulphide isotopic liquid solutions [13] in a thermogravitational column, although he predicts that in such systems there is also a positive rotational contribution to the thermomigration. This could be explained by the lack of reference data to calibrate their column, and surely by the physical differences of the systems.

The similarity, however, encouraged us to extend such an approach to all the systems measured in microgravity. How far it is possible to extend this approach to nonisotopic and condensed systems has not yet been assessed, mainly because the attempts in this direction have not considered many interaction potentials.

In order to improve the predictions for dense systems, Kincaid *et al.* developed [14] a theory for dense multicomponent systems, not necessarily dilute. They named their theory ''revised Enskog theory'' (RET). In the implementation of the RET that they proposed [15], binary interactions are modeled by hard core collisions and thermodiffusion and interdiffusion coefficients obtained by Sonine expansions also. The resulting expressions are combinations of microscopic quantities resulting from the collision integral of the Boltzman equation, and of derivatives with respect to composition of the chemical potentials. The appearance of such
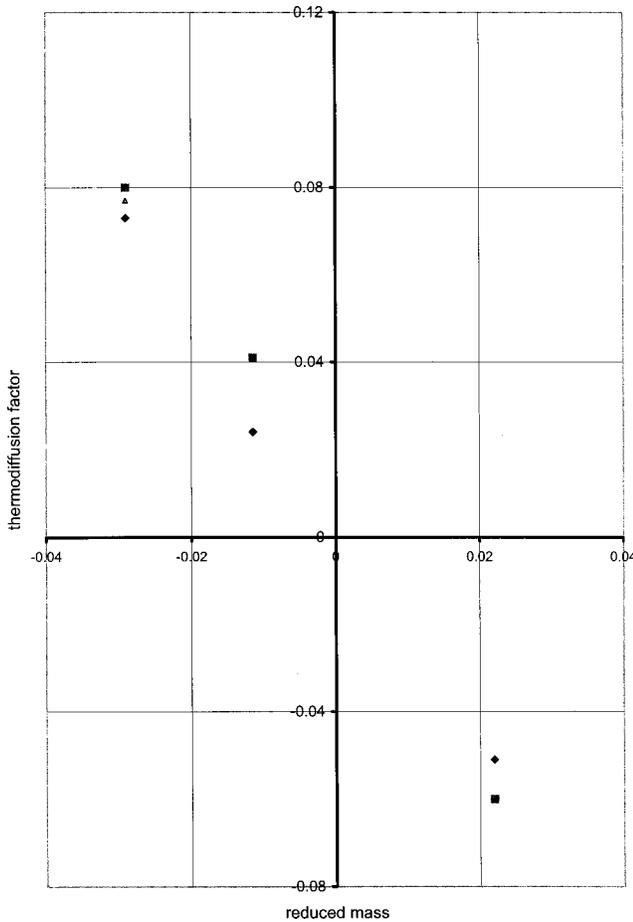
FIG. 1. Values of the thermodiffusion factors measured in the tin isotopes, as a function of their reduced mass. Squares: Eureca, capillary 3; losenges: Eureca, capillary 1; triangle: D1. From left to right appear the isotopes 112, 116, and 124.

quantities can be understood by considering the Onsager formalism [1] and inserting *stricto sensu* the generalized forces in the phenomenological expressions obtained by the kinetic theory [12].

In the case of diluted solutions, however, these derivatives reduce to compositional variables and the isothermal diffusive couplings, which may be very complex in nondiluted

multicomponents systems [16], are reduced to binary diffusion. We shall consider such an approximation to interpret the results because even with the simple hard core model of interaction potential, the expressions are very complex. One of the reasons, shown by Kincaid [15], is that to obtain a convergence of the development up to 1%, a seventh order Sonine expansion is required.

For isotopic mixtures at the tracer limit, they obtained numerically that the thermodiffusion factor of component 1 could be expanded in series of the reduced mass under the form

$$k_{T_1} = f(d)\mu(1 - g(d)(X_1 - X_2)\mu + \cdots), \qquad (8)$$

where X_i are the mole fractions and where f and g are functions only of the reduced density. The latter are defined with the density of atoms n and atomic diameter of solvent by

$$d = n\sigma^3. \qquad (9)$$

The value of g is between 0.22 and 0.18 when d varies between 0 and 0.5 and in these limits f varies increasingly between 105/118 and 0.44 [15].

The theory of Kincaid can be tested first with the group of Sn isotopes, and then with the other elements. The best fitting obtained with formula (8) for the group of Sn isotopes is a value of d of 0.25. For a density of liquid Sn of 7 g/cm^3 [17], this gives with formula (9) a diameter of the Sn particules of 1.78 Å. This value is to be compared to the atomic and ionic diameters given in [18] and reported in the seventh row of Table VI. We see that the Sn particules would appear under a form near Sn^{2+}.

Taking the same value of d (0.25), Kincaid's theory would give, for the other elements, values of thermodiffusion factors given in the fourth row of Table VI. These values are smaller than the ones observed.

It seems therefore that different values should be considered for each alloy, and this is done in the fifth row of Table VI. It gives for each alloy the value of d of Kincaid's theory that fits the best each single experimental result. From it, we deduce an "experimental diameter" by formula (9), as done for the Sn isotopes, using as density the one of the pure liquid Sn.

TABLE VI. The first column indicates the successive rows. The content of the successive rows are (1) the elements in solution in natural tin, (2) reduced mass, (3) experimental thermodiffusion factors obtained in microgravity, (4) theoretical value according to Kincaid's theory obtained with d fitting the best the isotope group, (5) best d to fit each specific measurement with Eq. (8), (6) atomic diameter resulting from previous row, and (7) ionic diameters according to [18]. The row (8) is the quantity of Eq. (10).

1	Co	Ag	^{112}Sn	^{116}Sn	^{124}Sn	Au	Bi
2	−0.336	−0.048	−0.029	−0.0115	0.022	0.248	0.276
3	1.860	0.175	0.077	0.024	−0.050	−0.574	−0.758
4	1.002	0.112	0.068	0.027	−0.051	−0.553	−0.611
5	0.55	0.34	0.26	0.22	0.27	0.30	0.35
6	2.50	2.12		1.93		2.04	2.14
7	Co 1.18	Ag 1.28		Sn 1.24		Au 2.38	Bi 2.58
	Co^{++} 0.68	Ag^{+} 0.1.06		Sn^{++} 1.98		Au^{+} 1.26	Bi^{3+} 1.86
	Co^{3+} 0.66	Ag^{++} 1.04					
8	−0.08	0.29				0.29	0.61

Contrary to pure Sn, the impurities are appearing with an apparent diameter close to the one of the nonionized form. The departure from the nonionized form can be characterized by the ratio

$$\frac{\sigma^{\text{experiment}} - \sigma^{\text{element}}}{\sigma^{\text{element}} - \sigma^{\text{first ion}}}. \tag{10}$$

This is performed in the eighth row of Table VI. This parameter appears to be well correlated with the position of the element in the Mendeleev table, that is, with the electronegativity scale. It is, however, difficult to infer more precise thermodynamical correlations.

In any case, the mean density of solvent cannot be considered as mean dimension for the alloys. It is likely that a short distance order at atomic scale and the electronic redistribution around inpurities modifies the thermodiffusive process with respect to the case of gazes.

B. Results of nonkinetic theories

A possible correction of the kinetic theory is due to the presence of an additional electronic contribution in metals. Fick and Huntington [19] have quantified by a semiclassical treatment the effect of elastic diffusion of conduction electron on impurities present in an homogeneous solid. Gerl [20] has considered later alloys where migrations happens through jumps of the impurities into vacancies. The mechanism that he proposed is a transport induced by the Coulombic interaction between the screened vacancies. In any case, the electronic contribution to the themodiffusion factor is proportional to the absolute temperature.

Extension to liquids of the mechanism proposed by Gerl has been performed by Balourdet [21] by introducing the structure factor of the pure solvent and determining the deviation of the electronic distribution with respect to equilibrium by the Born autocoherent first approximation. Combining the resulting actions on each component to the global action of the thermoelectric field, he obtains that the electronic contribution given by

$$k_T^{\text{el}} = BT, \tag{11}$$

where

$$B = Z \frac{\pi^2 k_B^2}{3 E_F} \left(\xi - \frac{\rho_i^{\text{el}}}{\rho^{\text{el}}} \xi_i \right). \tag{12}$$

This expression depends on the number of conduction electrons by atom (Z), on the Fermi energy (E_F), on partial and total electrical conductivities, and on the partial and total thermoelectric powers. The values obtained for B for several systems are reported on Table VII, with the resulting electronic contribution at 500 and 700 °C.

In any case it appears that the so computed electronic contribution would be significant enough to introduce an important temperature dependence of the thermodiffusion factor that has not been observed in microgravity measurements (see the standard deviations given in Table I). Furthermore, the consideration of such large contributions will provide higher discrepancies between Kincaid's theory and experiments.

TABLE VII. values of B [Eq. (11)] for different systems and the corresponding electronic contributions to the thermodiffusion factor.

Solvent	Ag	Au	Bi
$10^4 B$	1.638	2.036	−1.770
(K^{-1})			
BT	0.141	0.176	−0.137
(500 °C)			
$k_T^{\text{el}}/k_T^{\text{microg}}$	80.6%	−30.7%	18.1%
(500 °C)			
BT	0.178	0.221	−0.192
(700 °C)			
$k_T^{\text{el}}/k_T^{\text{microg}}$	101.7%	−38.5%	25.3%
(700 °C)			

This fact does not, however, demonstrate that the electronic contribution is negligible, but that the model used is too rough. Maybe that for the electronic contribution, the modification by impurities of the short order structure should also be considered.

C. Possible improvements of kinetic theory predictions

In both Kincaid's and Balourdet's results, the structure of fluid considered is the one of a pure condensed gas. This is obvious in Balourdet's theory by the explicit use of the structure factor of the pure solvent. In Kincaid's theory, this is more subtle, and not explicit, but the simple hard core model has surely not the impact on the structure of the fluid solutions that would have the real potential accounting among others for the short range dimensional effects.

A local ordering of the fluid, if effective, should globally decrease the entropy of the system in order to account for the separations larger than predicted by a condensed gas.

Also, the short order structure of the liquid may introduce contributions of phonons to the thermomigration. Note that a phononic theory as a full explanation of transport has been developed by Gaeta et al. [22]. It seems, however, at the present time difficult to fit the experimental results with it, essentially because of a lack of knowledge of the acousto-thermal quantities involved.

The same remark holds for the thermodynamic theory of Kempers [23], whereas anterior semiphenomenological thermodynamic theories do difficultly apply to metals.

Waiting for new and very accurate microgravity measurements to better assess the temperature dependence of the thermodiffusion factor, we need new guidelines to orient the theoretical research that may account for the observed values.

One possible way is to consider more complex potentials in the RET theory in order to account for all the interactions, including the nonclassical electronic and phononic contributions, although in a way in which they are not easily identified. There is unfortunately no such systematic studies performed on dense systems by the RET.

However, results obtained in gases may show what effect has the form of the interaction potential on the thermomigration. Such a systematic study has been performed first by Clark Jones in 1941 [24]. He considered the generalized

Lennard-Jones potentials for which the resulting spherically symmetric forces F are given as a function of interatomic distance r by

$$F = \frac{Cst}{r^n} - \frac{Cst'}{r^{n'}}. \tag{13}$$

It is counted positive when repulsive. A minimum in the potential energy-interatomic distance exists when $n > n'$ and is given in units of thermal agitation energy by

$$\frac{\epsilon}{k_B T} = \frac{n - n'}{(n-1)(n'-1)} \frac{Cst^{(n-1)/(n-n')}}{Cst'^{(n'-1)/(n-n')}}. \tag{14}$$

It can be easily verified with the results of [24] that a smoothed collision model provides a smaller temperature dependance for R than the hard core collisions and that large potential energy wells provide large values of R. The sensitivity of the Soret coefficients to the form of interaction potentials can be shown on the examples of inverse power model (n' infinite) and the (9,5) Lennard-Jones potential: The former provides values of R between 0.8 and 1, while the latter provides an inversion of the sign of R when the mean temperature is increased, with a negative value of R at low temperatures.

The fitting of the kinetic theory of dense gases could be improved also by the consideration of different Lennard-Jones potentials. If refined microgravity experiments were performed on a wide range of temperature, the validity of one of the Lennard-Jones models could be assessed, leading to valuable information on the interaction potentials.

V. CONCLUSIONS

The measurements of thermodiffusion factors obtained on samples processed in microgravity for the Au-Sn and pure Sn provide important data for the global evaluation of the measurements performed in microgravity in tin melts.

The data obtained on EURECA, thanks to the long microgravity period and to the very low level of acceleration perturbations, can be considered as reference measurements. It allows for the establishment of the modelling of convective effects in the shear cell technique and for developments in the field of condensed matter physics.

The good accuracy of the measurements is supported by the experimental verification of the isotopic thermomigration law (8) giving the mass dependence of the effect in condensed gases. As for the large amplitudes observed in isotopic mixtures and alloys of tin, a good fitting has been obtained with the nonequilibrium statistical theory of dense gazes using the hard core collision. Progress should be performed by considering other interaction potentials. There is a discrepancy between the theory of electronic contribution and experiment in that no convincing temperature dependence has been observed.

In any case, microgravity measurements lead to the conclusion, for the time being, that there is no possibility to consider complex interaction potentials or the electronic contribution. As for the existing thermodynamical and phononic theories, they cannot presently be used, because of lack of knowledge of the thermodynamical and acoustical quantities involved.

An explanation drawn with short order distance could improve the models, and be simulated by molecular dynamics. At the present time, there exists no molecular dynamics simulations for these metallic systems. However, if the electronic contribution is actually smaller than predicted, the physical models underlying the development of molecular dynamics will be the same as those as the basis of statistical theory and it is probable that mutual progress could be reached by the understanding of mechanisms of thermomigration.

[1] S. R. Degroot and P. Mazur, *Non-Equilibrium Thermodynamics* (North-Holland, Amsterdam, 1962).

[2] S. Van Vaerenbergh, J. C. Legros, and J. P. Praizey, Entropie **184-185**, 44 (1994).

[3] Y. Malmejac and J. P. Praizey, *Proceedings of the Fifth European Symposium on Material Sciences Under Microgravity, Schloss Elmau (RFA), 1984, ESA SP-222*, edited by T. D. Guyenne and J. Hunt (ESTEC Reproduction Service, Nordwijk, Netherlands), pp. 147–152.

[4] J. P. Praizey, Commissariat à L'Energie Atomique Report No. CEA-R-5449 (1988).

[5] J. P. Praizey, Int. J. Heat Mass Transf. **32**, 2385 (1989).

[6] J. P. Praizey, S. Van Vaerenbergh, and J. P. Garandet, Adv. Space Res. **16**, 205 (1995).

[7] S. Van Vaerenbergh, J. C. Legros, J. P. Praizey, and J. P. Garandet, Microgravity Q. **5**, 109 (1995).

[8] J. P. Garandet, C. Barat, J. P. Praizey, T. Duffar, and S. Van Vaerenbergh, *The Effect of Natural Convection in Liquid Phase Mass Transport Coefficients Measurements*, Lecture Notes in Physics Vol. 464 (Springer-Verlag, Berlin, 1996), pp. 253–260.

[9] J. P. Garandet, S. Van Vaerenbergh, J. P. Praizey, and T. Alboussière, Phys. Fluids **9**, 510 (1997).

[10] A. Bruson and M. Gerl, Phys. Rev. B **21**, 5447 (1980).

[11] S. Chapman and T. G. Cowling, *The Mathematical Theory of Nonuniform Gases* (Cambridge University Press, London, 1952).

[12] J. O. Hirschfelder, C. F. Curtiss, and R. B. Bird, *Molecular Theory of Gases and Liquids* (John Wiley & Sons, New York, 1965).

[13] W. M. Rutherford, J. Chem. Phys. **86**, 397 (1987).

[14] M. López de Haro, E. G. D. Cohen, and J. M. Kincaid, J. Chem. Phys. **78**, 2764 (1983).

[15] J. M. Kincaid, E. G. D. Cohen, and M. López de Haro, J. Chem. Phys. **86**, 963 (1986).

[16] Ross Taylor and R. Krishna, *Multicomponent Mass Transfer* (John Wiley & Sons, New York, 1954).

[17] Smithells, *Metal Reference Book*, 7th ed., edited by E. A. Brandes and G. B. Brook (Butterworth and Henemann, Oxford, 1992).

[18] G. V. Samsonov, *Handbook of the Physicochemical Properties of the Elements* (IFI/Plenum, New York, 1968).

[19] H. B. Huntington and A. R. Grone, J. Phys. Chem. Solids **20**, 76 (1961).

[20] M. Gerl, J. Phys. Chem. Solids **28**, 725 (1967).

[21] M. Balourdet, Ph.D. thesis, Grenoble, 1976 (unpublished).

[22] F. S. Gaeta, C. Albanese, D. G. Mitta, and F. Peluso, Phys. Rev. E **49**, 433 (1994).

[23] L. J. T. M. Kempers, J. Chem. Phys. **90**, 6541 (1989).

[24] R. Clark Jones, Phys. Rev. **58**, 111 (1940); **59**, 1019 (1941).